

Selective Coupling of Methylene Groups at a Rh/Os Core, Yielding C₂, C₃, or C₄ Fragments: Roles of the Adjacent Metals in Carbon–Carbon Bond Formation

Steven J. Trepanier, James N. L. Dennett, Brian T. Sterenberg,[†]
Robert McDonald,[‡] and Martin Cowie*

Contribution from the Department of Chemistry, University of Alberta Edmonton,
AB, Canada T6G 2G2

Received February 17, 2004; E-mail: martin.cowie@ualberta.ca

Abstract: The mixed-metal complex, [RhOs(CO)₄(dppm)₂][BF₄] (**1**; dppm = μ -Ph₂PCH₂PPh₂) reacts with diazomethane to yield a number of products resulting from methylene incorporation into the bimetallic core. At -80 °C the reaction between **1** and CH₂N₂ yields the methylene-bridged [RhOs(CO)₃(μ -CH₂)(μ -CO)-(dppm)₂][BF₄] (**2**), which reacts further at ambient temperature to give the allyl methyl species, [RhOs(η^1 -C₃H₅)(CH₃)(CO)₃(dppm)₂][BF₄] (**4**). At intermediate temperatures compounds **1** and **2** react with diazomethane to yield the butanediyli complex [RhOs(C₄H₈)(CO)₃(dppm)₂][BF₄] (**3**) by the incorporation and coupling of four methylene units. Compound **2** is proposed to be an intermediate in the formation of **3** and **4** from **1** and on the basis of labeling studies a mechanism has been proposed in which sequential insertions of diazomethane-generated methylene fragments into the Rh–C bond of bridging hydrocarbyl fragments occur. Reaction of the tricarbonyl species, [RhOs(CO)₃(μ -CH₂)(dppm)₂][BF₄] with diazomethane over a range of temperatures generates the ethylene complex [RhOs(η^2 -C₂H₄)(CO)₃(dppm)₂][BF₄] (**7a**), but no further incorporation of methylene groups is observed. This observation suggests that carbonyl loss in the formation of the above allyl and butanediyli species only occurs after incorporation of the third methylene fragment. Attempts to generate C₂-bridged species by the reaction of **1** with ethylene gave no reaction, however, in the presence of trimethylamine oxide the ethylene adducts [RhOs(η^2 -C₂H₄)(CO)₃(dppm)₂][BF₄] (**7b**; an isomer of **7a**) and [RhOs(η^2 -C₂H₄)₂(CO)₂(dppm)₂][BF₄] (**8**) were obtained. The relationship of the above products to the selective coupling of methylene groups, and the roles of the different metals are discussed.

Introduction

Despite the industrial successes of the Fischer–Tropsch (FT) reaction¹ since its discovery over 75 years ago,² the process is still not well understood and its lack of selectivity continues to be a drawback. Although there is general agreement that the reaction is a result of the stepwise polymerization of methylene groups,³ how this polymerization occurs is unknown and a number of mechanisms have been proposed, the most prominent of which involve either: the direct polymerization of methylene units (Fischer and Tropsch);² the coupling of methylene and alkyl fragments (Brady and Pettit; Biloen and Sachtler);⁴ the

coupling of methylene and vinyl groups (Maitlis et al.);⁵ or the coupling of methylene groups and surface-bound olefins (Dry).⁶ Significantly, all of these proposals involve methylene fragments bridging adjacent metal centers.

The observation that even within the closely related group 8 and 9 transition-metal catalysts, the different metals give substantially different products and product distributions,⁷ suggested to us that some control over product distributions might be achieved by the use of combinations of these metals. Certainly, improved selectivity has been reported for bimetallic catalysts over monometallic ones, as seen for example in hydrogenation reactions⁸ and in isomerization reactions of olefins.^{8,9} These ideas have also been applied to the FT process, where mixed Co/Ru catalysts have been investigated.¹⁰

Bimetallic catalysts clearly introduce additional complexity compared to single-metal systems and much remains to be

[†] Present address: Department of Chemistry, University of Regina, Regina, SK S4S 0A2.

[‡] X-ray Crystallography Laboratory.

- (1) (a) Pichler, H. *Adv. Catal.* **1952**, *4*, 271. (b) Jager, B.; Espinoza, R. *Catal. Today* **1995**, *23*, 17. (c) Van der Burgt, M.; van Klinken, J.; Sie, T. *The Shell Middle Distillate Synthesis Process*, 5th Synfuels Worldwide Symposium; Washington, DC, November 1985. (d) Haggin, J. *Chem. Eng. News* **1990**, 23rd July, 27.
- (2) (a) Fischer, F.; Tropsch, H. *Brennst.-Chem.* **1926**, *7*, 97. Fischer, F.; Tropsch, H. *Chem. Ber.* **1926**, *59*, 830.
- (3) Kaminsky, M. P.; Winograd, N.; Geoffroy, G. L.; Vannice, M. A. *J. Am. Chem. Soc.* **1986**, *108*, 1315.
- (4) (a) Brady, R.; Pettit, R. *J. Am. Chem. Soc.* **1980**, *102*, 6181. (b) Brady, R. C.; Pettit, R. *J. Am. Chem. Soc.* **1981**, *103*, 1287. (c) Biloen, P.; Sachtler, W. M. H. *Adv. Catal.* **1980**, *30*, 165.

- (5) (a) Maitlis, P. M.; Long, H. C.; Quyoum, R.; Turner, M. L.; Wang, Z.-Q. *Chem. Commun.* **1996**, *1*. (b) Long, H. C.; Turner, M. L.; Fornasiero, P.; Kaspar, J.; Graziani, M.; Maitlis, P. M. *J. Catal.* **1997**, *167*, 172.
- (6) Dry, M. E. *Appl. Catal. A: General* **1996**, *138*, 319.
- (7) Vannice, M. A. *J. Catal.* **1975**, *37*, 449.
- (8) Sinfelt, J. H. *Bimetallic Catalysts: Discoveries, Concepts and Applications*; Wiley: New York, 1983; Chapter 2.
- (9) da Silva, A. C.; Piotrowski, H.; Mayer, P.; Polborn, K.; Severin, K. *Eur. J. Inorg. Chem.* **2001**, 685.
- (10) Iglesia, E.; Soled, S. L.; Fiato, R. A.; Via, G. H. *J. Catal.* **1993**, *143*, 345.

learned about the roles of the different metals in these systems. We have adopted an approach of studying well defined, heterobinuclear complexes of groups 8 and 9 with a view toward determining the roles of the metals in processes of carbon–carbon bond formation. Our interest in the FT process and the established significance of bridging methylene groups in this chemistry prompted us to study the reactivity of complexes containing the $M(\mu\text{-CH}_2)M'$ core ($M = \text{Rh, Ir; } M' = \text{Ru, Os}$),^{11–13} and in this paper, we report our results on the unusually selective coupling of methylene groups at a Rh/Os core, a preliminary version of which has appeared.^{11a}

Experimental Section

General Comments. All solvents were deoxygenated, dried (using appropriate drying agents), distilled before use, and stored under nitrogen. Reactions were performed under an argon atmosphere using standard Schlenk techniques. $\text{RhCl}_3 \cdot x\text{H}_2\text{O}$ was purchased from Strem Chemicals, $\text{Os}_3(\text{CO})_{12}$ was purchased from Colonial Metals Inc., and Diazald (including ²H and ¹³C enriched) was purchased from Aldrich. ¹³C-enriched CO (99.4% enrichment) was purchased from Isotec Inc. and Cambridge Isotope Laboratories (99% enrichment). The compounds, $[\text{RhOs}(\text{CO})_4(\text{dppm})_2][\text{BF}_4]$ (**1**)¹⁴ and $[\text{RhOs}(\eta^3\text{-C}_3\text{H}_5)(\text{CO})_3(\text{dppm})_2]$ ¹⁵ were prepared by the published procedures.

NMR spectra were recorded on a Varian iNova-400 spectrometer operating at 400.1 MHz for ¹H, 161.9 MHz ³¹P, and 100.6 MHz for ¹³C nuclei. Infrared spectra were obtained on a Nicolet Magna 750 FTIR spectrometer with a NIC-Plan IR microscope. Spectroscopic data for all compounds appear in Table 1. The elemental analyses were performed by the microanalytical service within the department. Electrospray ionization mass spectra were run on a Micromass Zabspec spectrometer. In all cases, the distribution of isotope peaks for the appropriate parent ion matched very closely that calculated from the formulation given.

Preparation of Compounds. (a) $[\text{RhOs}(\text{CO})_4(\mu\text{-CH}_2)(\text{dppm})_2][\text{BF}_4]$ (**2**). The compound $[\text{RhOs}(\text{CO})_4(\text{dppm})_2][\text{BF}_4]$ (**1**) (100 mg, 0.079 mmol) was dissolved in 15 mL of CH_2Cl_2 and the solution cooled to -78°C in an acetone/dry ice bath. Gaseous diazomethane (ca. 18 equiv), generated from 300 mg (1.4 mmol) of Diazald, was passed through the solution for 30 min. The solution was kept at -78°C and put under dynamic vacuum for another 30 min. The cold bath was then removed and the reaction mixture was pumped to dryness, yielding a yellow residue. This residue was dissolved in 5 mL of CH_2Cl_2 and 30 mL of ether was added to precipitate a yellow solid. The solid was washed with 3×5 mL of ether and dried in vacuo (93 mg obtained, 92% yield). Anal. Calcd. for $\text{RhOsP}_4\text{F}_4\text{BO}_3\text{C}_5\text{H}_4$: C, 51.81; H, 3.64. Found: C, 51.63; H, 3.67. MS m/z 1188 ($M^+ - \text{BF}_4$)

(b) $[\text{RhOs}(\text{C}_4\text{H}_8)(\text{CO})_3(\text{dppm})_2][\text{BF}_4]$ (**3**). **Method (i).** The compound $[\text{RhOs}(\text{CO})_4(\mu\text{-CH}_2)(\text{dppm})_2][\text{BF}_4]$ (**2**) (50 mg, 0.039 mmol) was dissolved in 20 mL of CH_2Cl_2 and the solution cooled to -60°C . Diazomethane (ca. 15 equiv), generated from 500 mg (2.3 mmol) of Diazald, was passed through the solution for 1 h followed by stirring for an additional hour. The solution was then put under dynamic vacuum at -60°C for 1 h. The cold bath was then removed and the reaction mixture was pumped to dryness, yielding a yellow residue. This residue was dissolved in 5 mL of CH_2Cl_2 and 40 mL of ether was added to precipitate a yellow solid. The solid was washed with 3×5 mL of

ether and dried in vacuo (43 mg obtained, 85% yield). Anal. Calcd. for $\text{RhOsP}_4\text{F}_4\text{BO}_3\text{C}_7\text{H}_5$: C, 53.12; H, 4.07. Found: C, 52.81; H, 3.92. MS m/z 1202 ($M^+ - \text{BF}_4$).

Method (ii). The compound $[\text{RhOs}(\text{CO})_4(\text{dppm})_2][\text{BF}_4]$ (**1**) (50 mg, 0.040 mmol) was dissolved in 20 mL of CH_2Cl_2 and the solution cooled to -60°C . Diazomethane (ca. 15 equiv), generated from 500 mg (2.3 mmol) of Diazald, was passed through the solution for 1 h and the solution was stirred for an additional hour. The solution was then put under dynamic vacuum for 1 h. The cold bath was then removed and the reaction was pumped to dryness, yielding a yellow residue. This residue was dissolved in 5 mL of CH_2Cl_2 and 40 mL of ether was added to precipitate a yellow solid. The solid was washed with 3×5 mL of ether and dried in vacuo (42 mg obtained, 82% yield).

(c) $[\text{RhOs}(\eta^1\text{-C}_3\text{H}_5)(\text{CH}_3)(\text{CO})_3(\text{dppm})_2][\text{BF}_4]$ (**4**). **Method (i).** The compound $[\text{RhOs}(\text{CO})_4(\mu\text{-CH}_2)(\text{dppm})_2][\text{BF}_4]$ (**2**) (50 mg, 0.039 mmol) was dissolved in 5 mL of THF at ambient temperature. Diazomethane (ca. 12 equiv), generated from 100 mg (0.47 mmol) of Diazald, was passed through the solution for 15 min. 30 mL of ether was then added resulting in the precipitation of a yellow solid, which was washed with 3×5 mL of ether and dried in vacuo (43 mg obtained, 87% yield). Anal. Calcd. for $\text{RhOsP}_4\text{F}_4\text{BO}_3\text{C}_5\text{H}_5$: C, 51.99; H, 3.98. Found: C, 51.45; H, 3.35.

Method (ii). Compound **1** (50 mg, 0.040 mmol) was suspended in 15 mL of THF at ambient temperature. Diazomethane (ca. 12 equiv), generated from 100 mg (0.47 mmol) of Diazald, was passed through the solution for 15 min. The mixture was stirred for an additional 15 min, during which time the solution became clear. 50 mL of ether was added resulting in the precipitation of a yellow solid, which was washed with 3×5 mL of ether and dried in vacuo to give 41 mg of product (82% yield).

Method (iii). Compound **4** as the triflate salt was prepared by the addition of methyltriflate (4.8 μL , 0.042 mmol) to a solution of the compound $[\text{RhOs}(\text{CO})_3(\eta^3\text{-C}_3\text{H}_5)(\text{dppm})_2]$ (50 mg, 0.042 mmol) dissolved in 5 mL of THF. The solution was stirred for 30 min. 30 mL of ether was then added resulting in the precipitation of a yellow solid, which was washed with 3×5 mL of ether and dried in vacuo (89% yield).

(d) $[\text{RhOs}(\text{CO})_3(\mu\text{-CH}_2)(\text{dppm})_2][\text{BF}_4]$ (**5**). The compound $[\text{RhOs}(\text{CO})_4(\mu\text{-CH}_2)(\text{dppm})_2][\text{BF}_4]$ (**2**) (50 mg, 0.039 mmol) was dissolved in 4 mL of CH_2Cl_2 and Me_3NO (3.0 mg, 0.039 mmol), dissolved in 4 mL of CH_2Cl_2 , was then added to the solution, which immediately became orange. After stirring for 30 min the solution was concentrated to 4 mL under an argon stream, and 30 mL of ether was added to precipitate an orange solid. The solid was then washed with 3×5 mL of ether, recrystallized from CH_2Cl_2 /ether, and dried in vacuo (yield 77%). Satisfactory elemental analysis has not been obtained, however, mass spectral analysis confirmed the presence of **5**, which after purification was the only product detected by NMR spectroscopy. HRMS m/z . Calcd for $\text{RhOsP}_4\text{O}_3\text{C}_5\text{H}_4$: 1161.1067. Found: 1161.1064.

(e) $[\text{RhOs}(\text{CO})_3(\text{PMe}_3)(\mu\text{-CH}_2)(\text{dppm})_2][\text{BF}_4]$ (**6**). **Method (i).** Compound **2** (40 mg, 0.032 mmol) was dissolved in 5 mL of CH_2Cl_2 and 32 μL of a 1.0 M solution of PMe_3 in THF (0.032 mmol), was then added to the solution. The resulting yellow solution was stirred for 15 min and then concentrated to 3 mL under an argon stream. Ether (20 mL) was then added to precipitate a yellow solid which was washed with 3×10 mL of ether and dried in vacuo (yield 92%). Anal. Calcd for $\text{RhOsP}_5\text{F}_4\text{O}_3\text{BC}_5\text{H}_5$: C, 51.75; H, 4.19. Found: C, 51.42; H, 4.19. MS m/z 1236.0 ($M^+ - \text{BF}_4$).

Method (ii). Compound **5** (10 mg, 8 mmol) was dissolved in 0.7 mL of CD_2Cl_2 in an NMR tube sealed with a rubber septum. To this was added 8 μL of a 1.0 M solution of PMe_3 in THF (0.008 mmol) via syringe. Monitoring the resulting solution by ³¹P{¹H} and ¹H NMR spectroscopy confirmed that compound **6** was formed as the only observed phosphorus-containing product.

(f) $[\text{RhOs}(\eta^2\text{-C}_2\text{H}_4)(\text{CO})_3(\text{dppm})_2][\text{BF}_4]$ (**7a**). **Method (i).** Compound **5** (50 mg, 0.040 mmol) was dissolved in 10 mL of CH_2Cl_2 .

- (11) (a) Trepanier, S. J.; Sterenberg, B. T.; McDonald, R.; Cowie, M. *J. Am. Chem. Soc.* **1999**, *121*, 2613. (b) Trepanier, S. J.; McDonald, R.; Cowie, M. *Organometallics* **2003**, *22*, 2638.
 (12) (a) Rowsell, B. D.; Trepanier, S. J.; Lam, R.; McDonald, R.; Cowie, M. *Organometallics* **2002**, *21*, 3228. (b) Rowsell, B. D.; McDonald, R.; Ferguson, M. J.; Cowie, M. *Organometallics* **2003**, *22*, 2944.
 (13) Dell'Anna, M. M.; Trepanier, S. J.; McDonald, R.; Cowie, M. *Organometallics* **2001**, *20*, 88.
 (14) Hiltz, R. W.; Franchuk, R. A.; Cowie, M. *Organometallics* **1991**, *10*, 304.
 (15) Sterenberg, B. T.; McDonald, R.; Cowie, M. *Organometallics* **1997**, *16*, 2297.

Table 1. Spectroscopic Data for Compounds

compound	ir (cm ⁻¹) ^{a,b}		nmr ^{c,d}	
	$\delta^{31}\text{P}\{\text{H}\}^e$ (ppm)	$\delta^1\text{H}$ (ppm) ^{f,g}	$\delta^{13}\text{C}\{\text{H}\}$ (ppm) ^g	
[RhOs(CO) ₄ (μ -CH ₂)(dppm) ₂][BF ₄] (2)	2043 (s) 1970(s) 1798 (m)	P(Rh): 33.7 (dm, ¹ J _{RhP} = 157 Hz) P(Os): -2.8 (m)	μ -CH ₂ : 2.25 (m, 2H) dppm: 3.75 (m, 2H); 2.80 (m, 2H)	μ -CH ₂ : 32.8 (d, ¹ J _{RhC} = 15 Hz) CO(Os): 176.3 (br); 176.6 (t); μ -CO: 210.5 (dm, ¹ J _{RhC} = 26 Hz) CO(Rh): 195.0 (dt, ¹ J _{RhC} = 57 Hz) C ₄ H ₈ : 24.6 (d, ¹ J _{CC} = 31 Hz, C ₄); 36.2 (t, ¹ J _{CC} = 34 Hz, C ₅); 37.8 (t, ¹ J _{CC} = 33 Hz, C ₆); -0.3 (d, ¹ J _{CC} = 30 Hz, C ₇) CO(Os): 182.4 (dt, ² J _{PC} = 9 Hz, ² J _{CC} = 2 Hz); 191.1 (m) CO(Rh): 186.4 (ddt, ¹ J _{RhC} = 81 Hz, ² J _{CC} = 5 Hz, ² J _{PC} = 17 Hz) CO(Os): 179.1 (dt, ² J _{CC} = 27 Hz, ² J _{PC} = 9 Hz), 203.5 (dm, ¹ J _{RhC} = 12 Hz) μ -CO: 232.6 (ddm, ¹ J _{RhC} = 27 Hz, ² J _{CC} = 27 Hz) ^h
[RhOs(C ₄ H ₈)(CO) ₃ (dppm) ₂][BF ₄] (3)	1970 (s) 1850 (m)	P(Rh): 22.2 (dm, ¹ J _{RhP} = 106 Hz) P(Os): -6.7 (m)	C ₄ H ₈ : 0.67 (m, 2H ₄); 1.06 (m, 2H ₅); 2.09 (br, 2H ₆); 1.18 (br, 2H ₇) dppm: 3.80 (m, 2H); 3.93 (m, 2H) ^h	C ₄ H ₈ : 24.6 (d, ¹ J _{CC} = 31 Hz, C ₄); 36.2 (t, ¹ J _{CC} = 34 Hz, C ₅); 37.8 (t, ¹ J _{CC} = 33 Hz, C ₆); -0.3 (d, ¹ J _{CC} = 30 Hz, C ₇) CO(Os): 182.4 (dt, ² J _{PC} = 9 Hz, ² J _{CC} = 2 Hz); 191.1 (m) CO(Rh): 186.4 (ddt, ¹ J _{RhC} = 81 Hz, ² J _{CC} = 5 Hz, ² J _{PC} = 17 Hz) CO(Os): 179.1 (dt, ² J _{CC} = 27 Hz, ² J _{PC} = 9 Hz), 203.5 (dm, ¹ J _{RhC} = 12 Hz) μ -CO: 232.6 (ddm, ¹ J _{RhC} = 27 Hz, ² J _{CC} = 27 Hz) ^h
[RhOs(C ₃ H ₅)(CH ₃)(CO) ₃ (dppm) ₂][BF ₄] (4)	2031 (s) 1799 (m)	P(Rh): 27.3 (dm, ¹ J _{RhP} = 148 Hz) P(Os): -5.0 (m) ^h	CH ₃ : -0.26 (t, 3H, ³ J _{PH} = 7 Hz) C ₃ H ₅ : 2.60 (dm, 2H, ³ J _{HH} = 7 Hz); 2.89 (d, 1H, ³ J _{HH} = 16 Hz); 3.70 (d, 1H, ³ J _{HH} = 10 Hz); 5.16 (ddt, 1H, ³ J _{HH} = 16, 10 Hz, ² J _{HH} = 7 Hz) dppm: 3.23 (m, 2H), 3.33 (m, 2H) ^h 6.38 (tt, ³ J _{P(Os)H} = 13 Hz, ³ J _{P(Rh)H} = 8 Hz) 4.25 (m, 2H) 3.82 (m, 2H)	CH ₃ : -0.26 (t, 3H, ³ J _{PH} = 7 Hz) C ₃ H ₅ : 2.60 (dm, 2H, ³ J _{HH} = 7 Hz); 2.89 (d, 1H, ³ J _{HH} = 16 Hz); 3.70 (d, 1H, ³ J _{HH} = 10 Hz); 5.16 (ddt, 1H, ³ J _{HH} = 16, 10 Hz, ² J _{HH} = 7 Hz) dppm: 3.23 (m, 2H), 3.33 (m, 2H) ^h 6.38 (tt, ³ J _{P(Os)H} = 13 Hz, ³ J _{P(Rh)H} = 8 Hz) 4.25 (m, 2H) 3.82 (m, 2H)
[RhOs(CO) ₃ (μ -CH ₂)(dppm) ₂][BF ₄] (5)	1994 (s) 1937 (s)	P(Rh): 27.0 (m) P(Os): 2.1 (m)	6.38 (tt, ³ J _{P(Os)H} = 13 Hz, ³ J _{P(Rh)H} = 8 Hz) 4.25 (m, 2H) 3.82 (m, 2H)	dppm: 22.4 (m, 2C) μ -CH ₂ : 93.9 (s, br, 1C) CO(Os): 177.4 (dt, ² J _{RhC} = 4 Hz, ² J _{CP(Os)}} = 9 Hz); 186.7 (t, ² J _{CP(Os)}} = 5 Hz) CO(Rh): 189.7 (dt, ¹ J _{RhC} = 63 Hz, ² J _{CP(Rh)}} = 14 Hz) Me ₃ P: 18.02 (d, 3C, ¹ J _{PC} = 20 Hz) dppm: 26.1 (m, 2C) μ -CH ₂ : 75.9 (m, 1C) CO(Os): 181.4 (dt, ³ J _{CPMe₃} = 18 Hz, ² J _{CP(Os)}} = 14 Hz); 189.1 (dt, ³ J _{CPMe₃} = 2 Hz, ² J _{CP(Os)}} = 4 Hz) CO(Rh): 199.6 (ddt, ¹ J _{RhC} = 51 Hz, ² J _{CPMe₃} = 4 Hz, ² J _{CP(Rh)}} = 20 Hz) C ₂ H ₄ : 36.0 (s); 13.8 (s) CO(Os): 194.6 (m, br, ¹ J _{RhC} = 4 Hz); 184.6 (t, ² J _{PC} = 10 Hz) CO(Rh): 181.9 (dt, ¹ J _{RhC} = 74 Hz, ² J _{PC} = 17 Hz) C ₂ H ₄ : 64.2 (d, ¹ J _{RhC} = 11 Hz) CO(Os): 181.2 (t, 2C, ² J _{PC} = 13 Hz); 198.0 (dt, 1C, ¹ J _{RhC} = 6 Hz, ² J _{PC} = 9 Hz) CO(Os): 179.8 (br); 186.8 (br) CO(Rh): 194.3 (d, br, ¹ J _{RhC} = 60 Hz) ^h
[RhOs(CO) ₃ (PMe ₃)(μ -CH ₂)(dppm) ₂][BF ₄] (6)	1976 (s) 1960 (s) 1907 (s)	P(Rh): 18.2 (dm, ¹ J _{RhP} = 104 Hz) P(Os): -10.8 (m) PMe ₃ : -56.2 (dm, ¹ J _{RhP} = 117 Hz)	Me ₃ P: 0.75 (d, 9H, ² J _{PH} = 8 Hz) dppm: 3.53 (m, 2H); 4.31 (m, 2H) μ -CH ₂ : 4.88 (m, 2H)	Me ₃ P: 18.02 (d, 3C, ¹ J _{PC} = 20 Hz) dppm: 26.1 (m, 2C) μ -CH ₂ : 75.9 (m, 1C) CO(Os): 181.4 (dt, ³ J _{CPMe₃} = 18 Hz, ² J _{CP(Os)}} = 14 Hz); 189.1 (dt, ³ J _{CPMe₃} = 2 Hz, ² J _{CP(Os)}} = 4 Hz) CO(Rh): 199.6 (ddt, ¹ J _{RhC} = 51 Hz, ² J _{CPMe₃} = 4 Hz, ² J _{CP(Rh)}} = 20 Hz) C ₂ H ₄ : 36.0 (s); 13.8 (s) CO(Os): 194.6 (m, br, ¹ J _{RhC} = 4 Hz); 184.6 (t, ² J _{PC} = 10 Hz) CO(Rh): 181.9 (dt, ¹ J _{RhC} = 74 Hz, ² J _{PC} = 17 Hz) C ₂ H ₄ : 64.2 (d, ¹ J _{RhC} = 11 Hz) CO(Os): 181.2 (t, 2C, ² J _{PC} = 13 Hz); 198.0 (dt, 1C, ¹ J _{RhC} = 6 Hz, ² J _{PC} = 9 Hz) CO(Os): 179.8 (br); 186.8 (br) CO(Rh): 194.3 (d, br, ¹ J _{RhC} = 60 Hz) ^h
[RhOs(C ₂ H ₄)(CO) ₃ (dppm) ₂][BF ₄] (7a)	1959 (s), 1978 (s), 1906 (m, br)	P(Rh): 25.6 (dm, ¹ J _{RhP} = 116 Hz) P(Os): -5.5 (m)	C ₂ H ₄ : 2.13 (br, 2H); 1.12 (br, 2H) dppm: 3.95 (m, 2H); 3.58 (m, 2H)	C ₂ H ₄ : 36.0 (s); 13.8 (s) CO(Os): 194.6 (m, br, ¹ J _{RhC} = 4 Hz); 184.6 (t, ² J _{PC} = 10 Hz) CO(Rh): 181.9 (dt, ¹ J _{RhC} = 74 Hz, ² J _{PC} = 17 Hz) C ₂ H ₄ : 64.2 (d, ¹ J _{RhC} = 11 Hz) CO(Os): 181.2 (t, 2C, ² J _{PC} = 13 Hz); 198.0 (dt, 1C, ¹ J _{RhC} = 6 Hz, ² J _{PC} = 9 Hz) CO(Os): 179.8 (br); 186.8 (br) CO(Rh): 194.3 (d, br, ¹ J _{RhC} = 60 Hz) ^h
[RhOs(CO) ₃ (C ₂ H ₄)(dppm) ₂][BF ₄] (7b)	1985 (s) 1903 (s)	P(Rh): 33.1 (m) P(Os): -7.1 (m)	C ₂ H ₄ (Rh): 2.75 (m, 4H, ² J _{RhH} = 2 Hz) dppm: 4.04 (m, 4H)	C ₂ H ₄ : 64.2 (d, ¹ J _{RhC} = 11 Hz) CO(Os): 181.2 (t, 2C, ² J _{PC} = 13 Hz); 198.0 (dt, 1C, ¹ J _{RhC} = 6 Hz, ² J _{PC} = 9 Hz) CO(Os): 179.8 (br); 186.8 (br) CO(Rh): 194.3 (d, br, ¹ J _{RhC} = 60 Hz) ^h
[RhOs(C ₂ H ₄)(CO) ₃ (μ -CH ₂)(dppm) ₂][BF ₄] (8)		P(Rh): 26.7 (dm, ¹ J _{RhP} = 97 Hz) P(Os): -4.9 (m) ^h	dppm: 3.82 (br, 2H); 3.62 (br, 2H) C ₂ H ₄ : 4.95 (br, 4H) (μ -CH ₂): 5.88 (br, 2H) ^h	CO(Os): 179.8 (br); 186.8 (br) CO(Rh): 194.3 (d, br, ¹ J _{RhC} = 60 Hz) ^h
[RhOs(CO) ₂ (C ₂ H ₄) ₂ (dppm) ₂][BF ₄] (9)	1858 (s)	P(Rh): 32.7 (dm, ¹ J _{RhP} = 154 Hz) P(Os): 1.8 (m)	C ₂ H ₄ (Os): 0.90 (t, 4H, ³ J _{PH} = 6 Hz) C ₂ H ₄ (Rh): 2.89 (m, 4H, ² J _{RhH} = 2 Hz) dppm: 3.76 (m, 4H)	C ₂ H ₄ (Os): 23.5 (s, 2C) C ₂ H ₄ (Rh): 64.6 (d, 2C, ¹ J _{RhC} = 11 Hz) dppm: 34.5 (m, 2C) CO(Os): 195.5 (dt, 2C, ¹ J _{RhC} = ² J _{PC} = 8 Hz)

^a IR abbreviations: s = strong, m = medium. ^b Powder microscope. ^c NMR abbreviations: s = singlet, d = doublet, t = triplet, m = multiplet, br = broad. ^d NMR data at 25 °C in CD₂Cl₂. ^e ³¹P chemical shifts referenced to external 85% H₃PO₄. ^f Chemical shifts for the phenyl hydrogens not given. ^g ¹H and ¹³C chemical shifts referenced to TMS. ^h NMR data at -80 °C.

Diazomethane (ca. 25 equiv), generated from 200 mg (0.93 mmol) of Diazald, was passed through the solution for 5 min. The solution immediately changed from orange to yellow. After stirring for 30 min, the solution was concentrated to 5 mL under an argon stream and 30 mL of ether was added to precipitate a yellow solid (yield 83%). The solid was then washed with 3 × 5 mL of ether and dried in vacuo. HRMS *m/z*. Calcd for RhOsP₄O₃C₅₅H₄₈: 1175.1224. Found: 1175.1220.

Method (ii). The compound [RhOs(CO)₃(μ -CH₂)(dppm)₂][BF₄] **5** (10 mg, 0.008 mmol), dissolved in 0.7 mL of CD₂Cl₂, was sealed in

an NMR tube containing an ethylene atmosphere. After 3 days at room temperature approximately 80% of the sample had converted to [RhOs(η^2 -C₂H₄)(CO)₃(dppm)₂][BF₄] with the remainder being several uncharacterized species. Propene was also observed.

(g) [RhOs(η^2 -C₂H₄)(CO)₃(dppm)₂][BF₄] (7b). Compound **1** (80 mg, 0.064 mmol) was dissolved in 10 mL of CH₂Cl₂ and the solution placed under an ethylene atmosphere. Me₃NO (4.8 mg, 0.064 mmol), dissolved in 5 mL of CH₂Cl₂, was then added to the solution, which immediately became orange but after several minutes changed to yellow. After

Table 2. Crystallographic Data for Compounds **2** and **3**

	[RhOs(CO) ₄ (CH ₂)(dppm) ₂] [BF ₄] (2)	[RhOs(CO) ₃ (CH ₂) ₄ (dppm) ₂] [BF ₄] (3)
formula	C ₅₅ H ₄₆ BF ₄ O ₄ OsP ₄ Rh	C ₅₇ H ₅₂ BF ₄ O ₃ OsP ₄ Rh
fw	1274.72	1288.79
color	yellow-orange	pale yellow
cryst syst	monoclinic	monoclinic
space group	<i>I</i> 2/ <i>a</i> (an alternate setting of <i>C</i> 2/ <i>c</i> [No. 15])	<i>P</i> 2 ₁ / <i>n</i> (an alternate setting of <i>P</i> 2 ₁ / <i>c</i> [No. 14])
<i>a</i> , Å	42.751 (3) ^a	17.181 (1) ^b
<i>b</i> , Å	10.2233 (6)	12.1815 (7)
<i>c</i> , Å	23.580 (1)	26.533 (2)
β, deg	90.432 (1)	103.177 (1)
<i>V</i> , Å ³	10306 (1)	5406.7 (6)
<i>Z</i>	8	4
<i>d</i> _{calcd.} , g cm ^{−3}	1.643	1.583
<i>μ</i> , mm ^{−1}	2.968	2.828
<i>T</i> , °C	−80	−80
total data	24 873 (−52 ≤ <i>h</i> ≤ 53, −12 ≤ <i>k</i> ≤ 12, −29 ≤ <i>l</i> ≤ 10)	30 774 (−20 ≤ <i>h</i> ≤ 20, −14 ≤ <i>k</i> ≤ 5, −31 ≤ <i>l</i> ≤ 31)
no. of observns	8578 (<i>F</i> _o ² ≥ 2σ(<i>F</i> _o ²))	4930 (<i>F</i> _o ² ≥ 2σ(<i>F</i> _o ²))
<i>R</i> ₁ [<i>F</i> _o ² ≥ 2σ(<i>F</i> _o ²)]	0.0329	0.0675
<i>wR</i> ₂ (all data)	0.0744	0.1869

^a Cell parameters obtained from least-squares refinement of 5792 centered reflections. ^b Cell parameters obtained from least-squares refinement of 7295 centered reflections.

stirring for 30 min, the solution was concentrated to 5 mL under an argon stream and 30 mL of ether was added to precipitate a yellow solid. The solid was then washed with 3 × 5 mL of ether and dried in vacuo. The ³¹P NMR spectrum of this sample showed a mixture of compounds **1**, **7b**, and **9**; although variable amounts of the three compounds were obtained, typical ratios were ca. 1:3:2, respectively. A pure sample of **7b** could not be isolated, so characterization was based on NMR spectroscopy.

(h) [RhOs(η²-C₂H₄)(CO)₃(μ-CH₂)(dppm)₂][BF₄] (**8**). Compound **5** (10 mg, 0.008 mmol), dissolved in 0.7 mL of CD₂Cl₂, was sealed in an NMR tube containing an ethylene atmosphere. At room temperature only [RhOs(CO)₃(μ-CH₂)(dppm)₂][BF₄] was observed by NMR spectroscopy; however, upon cooling the sample to −80 °C complete conversion to the ethylene adduct (**8**) occurred. Warming the sample to room-temperature resulted in loss of ethylene and the reappearance of the starting complex **5**. Characterization of compound **8** was carried out by NMR spectroscopy (¹H, ¹³C, ³¹P) at −80 °C. After several days conversion to **7a** and propene was observed (see part (f), Method (ii)). Elemental analyses could not be obtained owing to facile loss of ethylene as described above.

(i) [RhOs(η²-C₂H₄)₂(CO)₂(dppm)₂][BF₄] (**9**). The compound [RhOs(CO)₄(dppm)₂][BF₄] (**1**) (80 mg, 0.064 mmol) was dissolved in 10 mL of CH₂Cl₂ and the solution placed under an ethylene atmosphere. Me₃-NO (9.6 mg, 0.13 mmol), dissolved in 5 mL of CH₂Cl₂, was then added to the solution, which immediately became orange but after several minutes changed to yellow. After stirring for 30 min, the solution was concentrated to 5 mL under an argon stream and 30 mL of ether was added to precipitate a yellow solid. The solid was then washed with 3 × 5 mL of ether and dried in vacuo (91% yield). Anal. Calcd for RhOsP₄F₄BO₂C₅₆H₅₂: C, 53.34; H, 4.16. Found: C, 53.08; H, 3.89. MS *m/z* 1174 (M⁺−BF₄).

(j) Reaction of Compound **3** with H₂. Dihydrogen was passed through an NMR tube containing [RhOs(C₄H₈)(CO)₃(dppm)₂][BF₄] (**3**) (10 mg, 0.008 mmol) dissolved in 0.7 mL of THF-*d*₈ for 30 s and the solution was left under an H₂ atmosphere. After approximately 8 h, 10% of the starting material had reacted, yielding the products [RhOs(CO)₃(μ-H)₂(dppm)₂][BF₄]¹⁴ and butane, observed by NMR spectroscopy. After 72 h, **3** had completely reacted, yielding these products. The dihydride product was readily identified by its ³¹P NMR resonances at δ 26.3 and −1.4 and the hydride resonance at δ −9.95.¹⁴

(k) Reaction of Compound **4** with H₂. Dihydrogen was passed through an NMR tube containing [RhOs(η¹-C₃H₅)(CH₃)(CO)₃(dppm)₂]-

[BF₄] (**4**) (10 mg, 0.008 mmol) dissolved in 0.7 mL of THF-*d*₈ for 30 s. After approximately 8 h, 15% of the starting material had reacted, yielding the products [RhOs(CO)₃(μ-H)₂(dppm)₂][BF₄],¹⁴ propene, and methane, as observed by NMR spectroscopy. After 72 h, the reaction was complete as judged by NMR spectroscopy.

X-ray Data Collection and Structure Solution

Yellow-orange crystals of [RhOs(CO)₃(μ-CH₂)(μ-CO)(dppm)₂]-[BF₄] (**2**) were obtained by slow diffusion of diethyl ether into a dichloromethane solution of the compound. Data were collected on a Bruker P4/RA/SMART 1000 CCD diffractometer¹⁶ using Mo Kα (λ = 0.710 73 Å) radiation at −80 °C. The data were corrected for absorption through use of the SADABS procedure. Unit cell parameters were obtained from a least-squares refinement of the setting angles of 5792 reflections from the data collection, and the space group was determined to be *I*2/*a* (an alternate setting of *C*2/*c* [No. 15]). See Table 2 for a summary of crystal data and X-ray data collection information.

Pale yellow crystals of [RhOs(CO)₃(C₄H₈)(dppm)₂][BF₄] (**3**) were obtained by slow diffusion of diethyl ether into a dichloromethane solution of the compound. Data were collected and corrected for absorption as for **2** above. Unit cell parameters were obtained from a least-squares refinement of the setting angles of 7295 reflections from the data collection. The space group was determined to be *P*2₁/*n* (an alternate setting of *P*2₁/*c* [No. 14]).

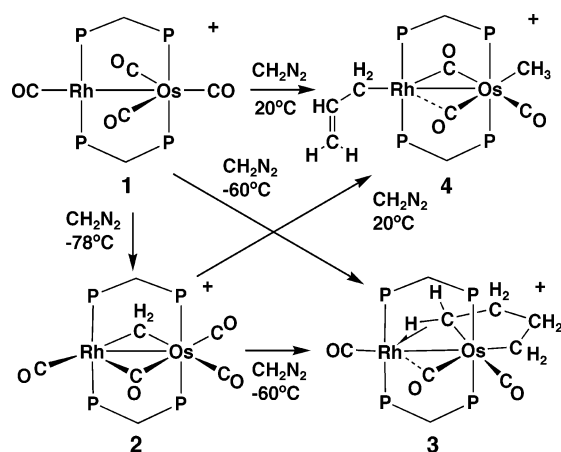
The structure of **2** was solved using the direct-methods program *SHELXS-86*,¹⁷ and refinement was completed using the program *SHELXL-93*.¹⁸ Hydrogen atoms were assigned positions based on the geometries of their attached carbon atoms, and were given thermal parameters 20% greater than those of the attached carbons. For **2** the boron and two fluorine atom positions for the tetrafluoroborate anion were found to be disordered; each of these atoms occupied two positions of half

(16) Programs for diffractometer operation, data collection, data reduction and absorption correction were those supplied by Bruker.

(17) Sheldrick, G. M. *Acta Crystallogr.* **1990**, *A46*, 467–473.

(18) Sheldrick, G. M. *SHELXL-93*, Program for crystal structure determination; University of Göttingen: Germany, 1993.

Scheme 1



occupancy and were refined independently. The final model for **2** was refined to values of $R_1(F) = 0.0329$ (for 8578 data with $F_o^2 \geq 2\sigma(F_o^2)$) and $wR_2(F^2) = 0.0744$ (for all 10 519 independent data).

The structure of **3** was solved as described for **2** and converged to $R_1(F) = 0.0675$ (for 4930 data with $F_o^2 \geq 2\sigma(F_o^2)$) and $wR_2(F^2) = 0.1869$ (for all 9864 independent data). The crystal quality of **3** was poorer than desired, even after many recrystallization attempts, leading to poorer data quality than ideal. Nevertheless, location of all non-hydrogen atoms proceeded without difficulty and refinement also proceeded uneventfully. The structure reported is based on the last (and best) of three data collections on samples obtained from different recrystallization attempts, that were carefully carried out with a full appreciation of the difficulties involved. Inspection of the thermal parameters suggested that one problem may arise from the flexibility within the C_4H_8 fragment giving rise to thermal parameters for these atoms that were larger than those of other atoms within the inner coordination sphere. Nevertheless, any disorder within this fragment must be slight since all atoms were well defined in electron density maps with no evidence of multiple positions. Furthermore, all bond lengths and angles within this group are normal.

Results and Compound Characterization

(a) Methylene Coupling Reactions. The mixed-metal complex $[RhOs(CO)_4(dppm)_2][BF_4]$ (**1**) ($dppm = \mu\text{-Ph}_2\text{PCH}_2\text{PPh}_2$) reacts with excess diazomethane at ambient temperature yielding essentially quantitatively the allyl- and methyl-containing product, $[RhOs(\eta^1\text{-CH}_2\text{CH}=\text{CH}_2)(\text{CH}_3)(\text{CO})_3(dppm)_2][BF_4]$ (**4**), through the incorporation of four methylene groups as shown in Scheme 1. The ^1H NMR spectrum of **4** shows the methyl resonance at $\delta -0.26$ as a triplet, due to spin-spin coupling to the Os-bound ends of the diphosphine ligands; the allyl protons are observed at δ 2.60 (2H), 2.89 (1H), 3.70 (1H), and 5.16 (1H). Selective ^{31}P decoupling experiments indicate that only the high-field pair of allyl hydrogens display coupling to the Rh-bound phosphorus nuclei, although no coupling of these α -protons to Rh is observed. Our failure to observe the two-bond Rh-H coupling is not unusual since such coupling to α -hydrogens is commonly less than 3 Hz. The β -hydrogen (δ 5.16) displays 7 Hz coupling to the α protons in addition to 10 Hz coupling to the cis and 16 Hz coupling to the trans olefinic hydrogens at δ 3.70 and 2.89, respectively. Further support for

the η^1 binding of the allyl group comes from the ^{13}C NMR spectrum of a sample of **4** prepared using $^{13}\text{CH}_2\text{N}_2$, in which only the α -carbon at δ 44.3 displays coupling (24 Hz) to Rh. The carbonyl groups in the ^{13}C NMR spectrum appear at δ 179.1, 203.5, and 232.6. While the high-field shift of the first resonance and its absence of Rh coupling establishes that this carbonyl is terminally bound to Os, the other two carbonyls are involved in some type of bridging interaction. We propose that the low-field carbonyl, which displays 27 Hz coupling to Rh, approximates a conventional bridging carbonyl, whereas the intermediate chemical shift of the other and its 12 Hz coupling to Rh indicate a weak semi-bridging interaction with this metal, as diagrammed in Scheme 1. Spin-saturation-transfer experiments at ambient temperature, in which irradiation of the α protons of the allyl group results in loss of the signal corresponding to the γ -protons, indicate that the allyl group is fluxional, alternating coordination to Rh by the α and γ carbons.

Compound **4** (as the triflate salt) can also be generated by the reaction of the known allyl complex, $[RhOs(\eta^3\text{-C}_3\text{H}_5)(\text{CO})_3(dppm)_2]$,¹⁵ with methyl triflate, adding further support for its formulation. Interestingly, methylation at the Os center of the η^3 -allyl precursor results in conversion of this allyl group to an η^1 coordination mode, presumably a consequence of the increase in coordination number and concomitant increase in steric crowding in the product.

In an attempt to learn more about this unprecedented conversion of diazomethane-generated methylene groups to an allyl and a methyl ligand we attempted to observe intermediates in this transformation by carrying out the reaction at lower temperatures. At -78°C , the reaction of **1** with diazomethane results in the exclusive formation of the methylene-bridged complex $[RhOs(\text{CO})_4(\mu\text{-CH}_2)(dppm)_2][BF_4]$ (**2**), which can be isolated in high yield by first removing the excess diazomethane before warming to ambient temperature. The $^{13}\text{C}\{^1\text{H}\}$ NMR spectrum of **2** shows four carbonyl resonances. Two of these, at δ 176.3 and 176.6, are in the characteristic range for carbonyls terminally bound to osmium and this has been confirmed by selective ^{31}P NMR decoupling experiments in which selective decoupling of the Os-bound ^{31}P nuclei results in collapse of these signals from triplets to singlets. The signal at δ 195.0 represents a rhodium-bound carbonyl as determined by selective ^{31}P NMR decoupling experiments and by the Rh-C coupling constant ($^1J_{\text{Rh-C}} = 57$ Hz) which is typical of such groups, and the resonance at δ 210.5 is in the characteristic range for bridging or semi-bridging carbonyls. $^{13}\text{C}\{^{31}\text{P}\}$ NMR spectroscopy, which shows coupling of this last carbonyl to all ^{31}P nuclei, allows us to confirm the bridging mode of this group, and the 26 Hz coupling of this carbonyl carbon to Rh is also typical of bridging carbonyls. Its bridging geometry is also confirmed by the IR spectrum, which shows a low-frequency stretch at 1798 cm^{-1} .

In the ^1H NMR spectrum the methylene group appears as a pseudo-quintet at δ 2.25 having essentially equal coupling to all four ^{31}P nuclei, confirming that it bridges the metals. No coupling of the methylene protons to Rh is evident. In the $^{13}\text{C}\{^1\text{H}\}$ NMR spectrum this methylene carbon appears at δ 32.8 and displays a coupling of 15 Hz to Rh, but no coupling to the Rh-bound phosphines is observed.

The geometry of **2** has been confirmed by an X-ray structure determination and a representation of the cation is shown in

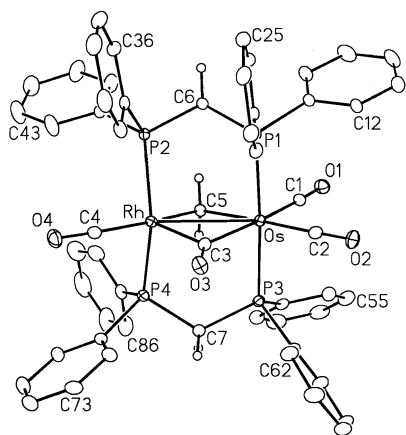


Figure 1. Perspective view of the complex cation of $[\text{RhOs}(\text{CO})_3(\mu\text{-CH}_2)(\mu\text{-CO})(\text{dppm})_2][\text{BF}_4]$ (**2**) showing the atomic labeling scheme. Numbering of the phenyl carbons starts at the ipso carbon and proceeds sequentially around the ring. Non-hydrogen atoms are represented by Gaussian ellipsoids at the 20% probability level, except for hydrogen atoms, which are shown arbitrarily small. Phenyl hydrogens are omitted.

Table 3. Selected Distances and Distances and Angles for Compound **2**

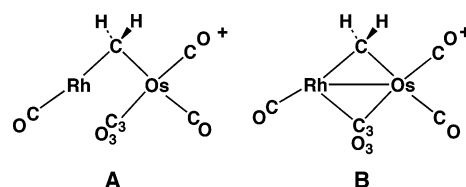
(a) distances (Å)					
atom 1	atom 2	distance	atom 1	atom 2	distance
Os	Rh	2.9413(4)	Rh	P(4)	2.301(1)
Os	P(1)	2.3867(9)	Rh	C(3)	2.027(4)
Os	P(3)	2.389(1)	Rh	C(4)	1.895(4)
Os	C(1)	1.907(4)	Rh	C(5)	2.088(4)
Os	C(2)	1.917(4)	O(1)	C(1)	1.150(5)
Os	C(3)	2.157(4)	O(2)	C(2)	1.143(5)
Os	C(5)	2.210(4)	O(3)	C(3)	1.163(5)
Rh	P(2)	2.3483(9)	O(4)	C(4)	1.144(5)

(b) angles (deg)							
atom 1	atom 2	atom 3	angle	atom 1	atom 2	atom 3	angle
P(1)	Os	P(3)	174.42(3)	C(3)	Rh	C(5)	94.9(2)
C(1)	Os	C(2)	94.4(2)	C(4)	Rh	C(5)	169.1(2)
C(1)	Os	C(3)	173.6(2)	Os	C(3)	Rh	89.3(2)
C(1)	Os	C(5)	85.6(2)	Os	C(3)	O(3)	141.7(3)
C(2)	Os	C(3)	92.0(2)	Rh	C(3)	O(3)	128.9(3)
C(2)	Os	C(5)	177.8(1)	Os	C(5)	Rh	86.3(1)
C(3)	Os	C(5)	88.0(1)	P(1)	C(6)	P(2)	110.0(2)
P(2)	Rh	P(4)	156.69(4)	P(3)	C(7)	P(4)	121.2(2)
C(3)	Rh	C(4)	95.5(2)				

Figure 1 with important bond lengths and angles given in Table 3. The geometry is typical of bis-dppm-bridged binuclear complexes, having both diphosphines in essentially trans arrangements at each metal, although the phosphines on Rh are bent back significantly ($\text{P}(2)\text{-Rh-P}(4) = 156.69(4)^\circ$) compared to those on Os ($\text{P}(1)\text{-Os-P}(3) = 174.42(3)^\circ$).

If the metal–metal bond is ignored, the geometry about Rh can be described as a tetragonal pyramid having the phosphines, the methylene, and the terminal carbonyl group in the basal sites, with the bridging carbonyl in the apical site. This description of Rh as a tetragonal pyramid is consistent with the bending back of the phosphines as described above. Similarly, the other atoms in the basal plane, C(4) and C(5), are also bent away from the apical site ($\text{C}(4)\text{-Rh-C}(5) = 169.1(2)^\circ$). The geometry at Os (also ignoring the metal–metal bond) is pseudo-octahedral with all angles between adjacent ligands close to 90° . The Rh–Os separation ($2.9413(4)\text{Å}$) is intermediate between what one would expect for a normal single bond (ca. $2.7\text{--}2.8$

Chart 1



Å)^{14,19} and a nonbonded separation ($>3.1\text{Å}$)¹⁹ and leaves some uncertainty in the nature of this interaction. Two valence-bond extremes can be proposed for a compound having the formulation of **2**, as shown in Chart 1. In the one extreme (**A**) the carbonyl labeled C(3)O(3) is terminally bound to Os, leaving Rh with a 16-electron configuration and Os with an 18-electron count. This formulation would not be expected to have a conventional Rh–Os bond. In the second extreme (**B**) carbonyl C(3)O(3) has a conventional bridging geometry and an accompanying Rh–Os bond, giving both metals an 18-electron configuration. Although carbonyl C(3)O(3) is clearly bridging, the other parameters indicate that the observed geometry appears to fall somewhere between these two extremes, albeit closer to extreme **B**. As a consequence, the metal–metal separation is, as noted above, intermediate between a conventional single bond and a nonbonded separation. Carbonyl C(3)O(3) is asymmetrically bridging ($\text{Os-C}(3)\text{-O}(3) = 141.7(3)^\circ$; $\text{Rh-C}(3)\text{-O}(3) = 128.9(3)^\circ$) and appears to be more strongly bound to Rh than to Os ($\text{Rh-C}(3) = 2.027(4)\text{Å}$; $\text{Os-C}(3) = 2.157(4)\text{Å}$). The lengthening of the Os–C(3) bond may result from the high trans influence of carbonyl C(1)O(1). Surprisingly perhaps, the bridging methylene group is also more strongly bound to Rh ($\text{Rh-C}(5) = 2.088(4)\text{Å}$; $\text{Os-C}(5) = 2.210(4)\text{Å}$).

The allyl/methyl product (**4**) can also be obtained by the reaction of the methylene-bridged compound $[\text{RhOs}(\text{CO})_4(\mu\text{-CH}_2)(\text{dppm})_2][\text{BF}_4]$ (**2**) with diazomethane at ambient temperature, suggesting that **2** could be an intermediate in the formation of **4**. This view is supported by subsequent labeling studies (vide infra).

The reaction of either compound **1** or **2** with excess diazomethane at between $-60\text{ }^\circ\text{C}$ and $-40\text{ }^\circ\text{C}$ yields a third product of methylene incorporation, $[\text{RhOs}(\text{C}_4\text{H}_8)(\text{CO})_3(\text{dppm})_2][\text{BF}_4]$ (**3**), in which the “condensation” of four intact methylene units has occurred forming an osmacyclopentane moiety (Scheme 1). The geometry of **3** has also been established by an X-ray structure determination and a representation of the complex cation (in which only the ipso carbons of the phenyl groups are shown) is presented in Figure 2. Important bond lengths and angles are given in Table 4. Again, as in compound **2**, the Rh–Os separation is long ($2.956(1)\text{Å}$) and suggests a weak interaction between the metals. The butanediyl fragment chelates to Os, having normal Os–C distances ($\text{Os-C}(4) = 2.20(1)\text{Å}$, $\text{Os-C}(7) = 2.30(1)\text{Å}$) and a bite angle of $79.3(4)^\circ$. Within this hydrocarbyl fragment the C–C distances ($1.45(2)\text{--}1.53(1)\text{Å}$) are normal for single bonds between sp^3 -hybridized carbons, as are the angles at these carbons ($103.8(7)^\circ\text{--}113(1)^\circ$). Although the hydrogen atoms were not located in this X-ray study, their positions have been idealized based on the geometries about their attached carbon atoms. This places H(7B) in close proximity to Rh (ca. 1.93Å), suggesting an agostic interaction

(19) Iggo, J. A.; Markham, D. P.; Shaw, B. L.; Thornton-Pett, M. *J. Chem. Soc., Chem. Commun.* **1985**, 432.

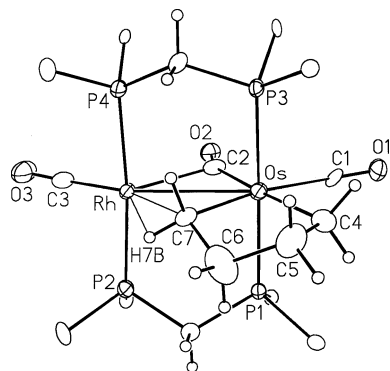


Figure 2. Perspective view of the complex cation of $[\text{RhOs}(\text{C}_4\text{H}_8)(\text{CO})_3\text{-(dppm)}_2][\text{BF}_4]$ (**3**) showing the atomic labeling scheme. Only the ipso carbons of the phenyl rings are shown. Thermal ellipsoids as described in Figure 1.

Table 4. Selected Distances and Angles of Compound **3**.

(a) distances (Å)					
atom 1	atom 2	distance	atom 1	atom 2	distance
Os	Rh	2.956(1)	Rh	C(3)	1.82(2)
Os	P(1)	2.392(3)	Rh	C(7)	2.46(1)
Os	P(3)	2.392(3)	Rh	H(7B)	1.93
Os	C(1)	1.90(2)	O(1)	C(1)	1.12(2)
Os	C(2)	2.03(1)	O(2)	C(2)	1.10(1)
Os	C(4)	2.20(1)	O(3)	C(3)	1.13(2)
Os	C(7)	2.30(1)	C(4)	C(5)	1.45(2)
Rh	P(2)	2.335(4)	C(5)	C(6)	1.51(2)
Rh	P(4)	2.343(4)	C(6)	C(7)	1.53(1)
Rh	C(2)	2.41(2)			

(b) angles (deg)							
atom 1	atom 2	atom 3	angle	atom 1	atom 2	atom 3	angle
P(1)	Os	P(3)	175.7(1)	Os	C(2)	O(2)	156(1)
C(1)	Os	C(2)	94.6(6)	Rh	C(2)	O(2)	121(1)
C(1)	Os	C(4)	78.1(5)	Os	C(4)	C(5)	113(1)
C(1)	Os	C(7)	157.2(5)	C(4)	C(5)	C(6)	112(1)
C(2)	Os	C(4)	172.5(6)	C(5)	C(6)	C(7)	112(1)
C(2)	Os	C(7)	108.1(5)	Os	C(7)	Rh	76.8(4)
C(4)	Os	C(7)	79.3(4)	Os	C(7)	C(6)	103.8(7)
P(2)	Rh	P(4)	174.5(1)	Rh	C(7)	C(6)	153.9(9)
Os	C(2)	Rh	83.0(6)				

of C(7)H(7B) with this metal. This interaction is supported by the Rh–C(7) distance (2.46(1) Å) which is typical of such an interaction^{20,21} and has been confirmed in solution by NMR studies (vide infra). The carbonyl C(2)O(2) is bound as a semibridging group in which the more linear arrangement involving its interaction with osmium (Rh–C(2)–O(2) = 121(1)°, Os–C(2)–O(2) = 156(1)°) correlates with the shorter metal–carbonyl distance (Os–C(2) = 2.03(1) Å, Rh–C(2) = 2.41(2) Å).

NMR characterization of **3** confirms that the geometry observed in the crystal is maintained in solution. The ¹H NMR spectrum of **3** displays four methylene resonances for the osmacyclopentane group, and the connectivity of the methylenes has been established using selective ¹H{³¹P} NMR spectroscopy and ¹H/¹H HMQC experiments. Unlike the solid-state structure, in which the agostic interaction involving H(7B) clearly differentiates it from uncoordinated H(7A), the solution NMR study shows only one broad resonance for both hydrogens

suggesting that a fluxional process interchanges them. We had assumed that the hydrogens that are involved in the agostic interaction would resonate at higher-field than the other methylene protons in the butanediyl moiety; however, an inspection of Table 1 shows that this not the case. Nevertheless, labeling studies establish the existence of this interaction. If compound **3** is generated from **1** by reaction with ¹³CH₂N₂, the ¹H NMR resonance at δ 1.18 shows a carbon–hydrogen coupling of 112 Hz. This is significantly less than the values observed for the other methylenes of the butanediyl group, ranging from 127 to 133 Hz. If, as suggested, both hydrogens of the “agostic” methylene group are alternating between an agostic and a terminal C–H bond, then the C–H coupling observed will be the average of the two. Assuming a value of ¹J_{CH} = 130 Hz for the terminal bond, the value for the agostic C–H bond is calculated from the average to be 94 Hz, consistent with previous reports.²¹

Further evidence for the agostic interaction comes from the ¹³C NMR spectrum, in which the resonance for C(7) appears at δ –0.3 (the ¹³C resonances are correlated to their attached protons using ¹H/¹³C HMQC spectroscopy), which is considerably upfield from the other ring carbons (δ 24.6, 36.2, 37.8) possibly indicating an additional interaction with the electron-rich rhodium center. Surprisingly, no coupling of this carbon to Rh is observed. Also observed in the ¹³C NMR spectrum are three carbonyl resonances. The one at δ 186.4 is assigned to a Rh-bound carbonyl on the basis of selective ¹³C{³¹P} NMR spectroscopy and a strong coupling of this carbon to rhodium (¹J_{Rh–C} = 81 Hz), the signal at δ 182.4 is due to a terminally bound osmium carbonyl, and the remaining resonance at δ 191.1 is due to a semi-bridging carbonyl. Although no Rh coupling to the latter carbonyl was resolved in the ¹³C NMR spectrum owing to the complexity of the signal, the semi-bridging formulation is supported by a carbonyl stretch at 1850 cm^{–1} in the IR spectrum. In any case, the X-ray structure determination confirms this assignment in the solid state.

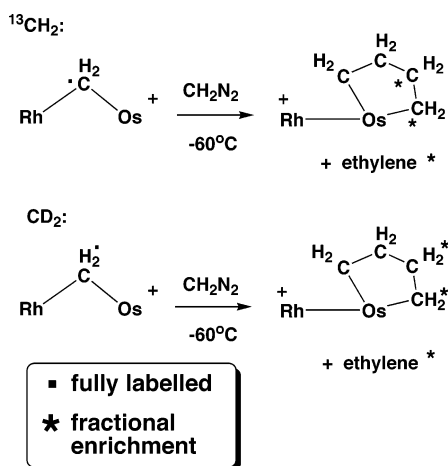
The reaction of **2** with diazomethane at –60 °C yields **3** exclusively, however, at increasing temperatures increasing amounts of **4** become evident. At –40 °C, compounds **4** and **3** appear in an approximate 1:50 ratio, whereas reactions at higher temperatures yield higher ratios of **4** and by ambient temperature only this species is observed. Warming a sample of **3** to ambient temperature does not result in its conversion to **4**, indicating that both products are derived by competing independent paths.

In an effort to obtain mechanistic information on the transformations of **2** into either **3** or **4**, the reactions of [RhOs(CO)₄(μ-CD₂)(dppm)₂][BF₄] (**2-D**₂) and [RhOs(CO)₄(μ-¹³CH₂)(dppm)₂][BF₄] (**2-¹³C**) with unlabeled CH₂N₂ have been monitored, to determine the sites of isotope incorporation in the products. In compound **3**, synthesized from either **2-¹³C** or **2-D**₂ at –60 °C, the ¹³C or deuterium label is scrambled equally between the two adjacent sites of the butanediyl moiety, remote from Rh, with none appearing in the other sites, as shown in Scheme 2. The reaction of CH₂N₂ with (**2-¹³C**) at ambient temperature yields **4**, in which the allyl group is ¹³C enriched in a 1:2:1 proportion at the α, β and γ positions, respectively, with no ¹³C incorporation into the methyl group (see Scheme 3). In the reaction of **2-D**₂ with unlabeled CH₂N₂, deuterium incorporation into all sites of the allyl and methyl groups of **4** is observed (vide infra). There is no evidence of deuterium

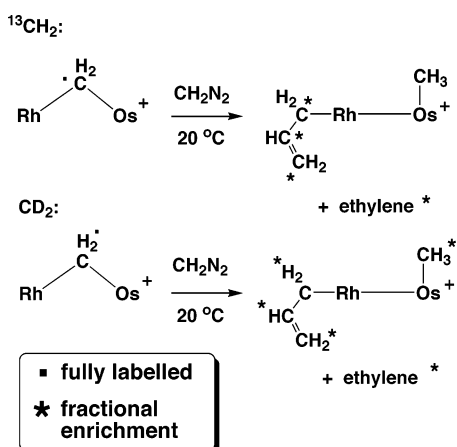
(20) Brookhart, M.; Green, M. L. H. *J. Organomet. Chem.* **1983**, *250*, 395.

(21) Brookhart, M.; Green, M. L. H.; Wong, L.-L. *Prog. Inorg. Chem.* **1988**, *36*, 1.

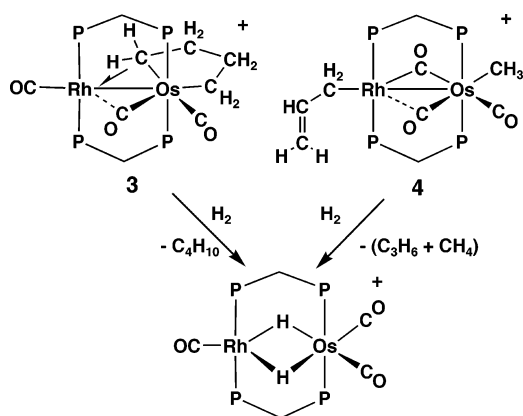
Scheme 2



Scheme 3



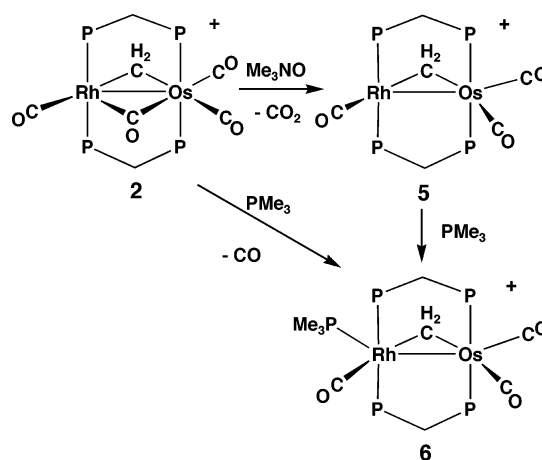
Scheme 4



incorporation into the dppm ligand of either product **3** or **4**. In Schemes 2 and 3 only the metals and the relevant hydrocarbyl fragments are shown. In both reactions, at -60°C and 25°C , with either $2\text{-}^{13}\text{C}$ or 2-D_2 , ^{13}C - or ^2H -enriched ethylene is observed as an additional product. On the basis of the labeling studies, a reaction sequence that rationalizes the selective formation of products **3** or **4** is proposed and will be explained in the Discussion section.

Both complexes **3** and **4** react slowly with H_2 , undergoing hydrogenolysis of the metal-alkyl bonds as shown in Scheme 4. In the reaction of **3** with H_2 the products obtained are the known dihydride complex $[\text{RhOs}(\text{CO})_3(\mu\text{-H})_2(\text{dppm})_2][\text{BF}_4]^{14}$

Scheme 5



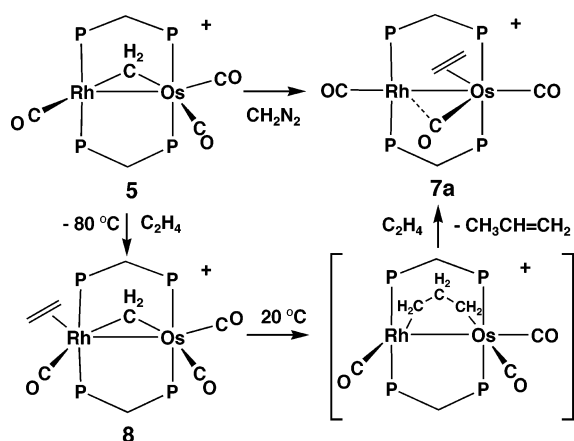
together with *n*-butane, whereas the reaction of **4** yields the same dihydride complex along with propene and methane. Interestingly, this dihydride product can in turn be converted to $[\text{RhOs}(\text{CO})_4(\text{dppm})_2][\text{BF}_4]$ (**1**) via addition of CO, and this complex can subsequently be transformed into either the osmacyclopentane complex (**3**) or allyl/methyl complex (**4**) by addition of CH_2N_2 at the appropriate temperatures. Regeneration of the starting hydrocarbyl species **3** and **4** allows us to construct a pseudo-catalytic cycle for the selective formation of butane, or methane and propene, from diazomethane and hydrogen.

Reaction of $[\text{RhOs}(\text{CO})_3(\mu\text{-CH}_2)(\mu\text{-CO})(\text{dppm})_2][\text{BF}_4]$ (**2**) with Me_3NO results in the loss of a carbonyl to give $[\text{RhOs}(\text{CO})_3(\mu\text{-CH}_2)(\text{dppm})_2][\text{BF}_4]$ (**5**) as shown in Scheme 5. ^1H NMR spectroscopy confirms that the methylene group remains bridging, appearing as a triplet of triplets at δ 6.38 owing to coupling with both sets of ^{31}P nuclei; as with the precursor (**2**) no spin–spin coupling between the methylene protons and Rh is observed. Three resonances to terminal carbonyl ligands are observed at δ 189.7, 186.7, and 177.4. The first displays 63 Hz coupling to Rh, clearly identifying that it is bound to this metal, whereas the other two display coupling to the Os-bound ends of the diphosphines. The high-field signal also displays 4 Hz coupling to Rh, consistent with it occupying a site on Os opposite the Rh–Os bond. This assignment is consistent with the upfield shift of this carbonyl in the ^{13}C NMR spectrum, compared to the other osmium-bound carbonyl, which is cis to the Rh–Os bond. We have previously noted²² that carbonyls cis to the metal–metal bond, therefore in closer proximity to the adjacent metal, display low-field ^{13}C chemical shifts.

(b) **PMe₃ Addition to Compound 2.** $[\text{RhOs}(\text{CO})_3(\mu\text{-CH}_2)(\mu\text{-CO})(\text{dppm})_2][\text{BF}_4]$ (**2**) reacts readily with PMe_3 yielding $[\text{RhOs}(\text{CO})_3(\text{PMe}_3)(\mu\text{-CH}_2)(\text{dppm})_2][\text{BF}_4]$ (**6**) quantitatively, accompanied by the loss of a carbonyl (Scheme 5). Compound **6** can also be synthesized by the addition of PMe_3 to the tricarbonyl compound $[\text{RhOs}(\text{CO})_3(\mu\text{-CH}_2)(\text{dppm})_2][\text{BF}_4]$ (**5**). The $^{31}\text{P}\{^1\text{H}\}$ NMR spectrum of **6** displays multiplets at δ 18.2 and -10.8 , typical of the rhodium- and osmium-bound dppm groups, respectively, as well as a high-field doublet of multiplets at δ -56.2 due to the PMe_3 group. The large rhodium coupling ($^1J_{\text{RhP}} = 117$ Hz) to this phosphine clearly identifies that the PMe_3 group is bound to rhodium. In the ^1H NMR spectrum,

(22) George, D. S. A.; McDonald, R.; Cowie, M. *Organometallics* **1998**, *17*, 2553.

Scheme 6



the bridging methylene group appears as a multiplet at δ 4.88 and selective ^{31}P decoupling experiments show coupling to all five ^{31}P nuclei. Also bound to rhodium is a carbonyl which resonates at δ 199.6 in the ^{13}C NMR spectrum ($^1J_{\text{RhP}} = 51\text{ Hz}$). Two other carbonyls, terminally bound to osmium, are observed at δ 181.4 and 189.1. Although one carbonyl in the isoelectronic precursor (**2**) is bridging, all carbonyls in **6** are terminally bound. Similar structures have been observed in the analogous Ir/Ru 13 and Rh/Ru 12a compounds, the structures of which have been confirmed by X-ray crystallography. Based on steric arguments, we would have expected **6** to have a structure like that of **2** in which the larger PMe_3 group would favor a carbonyl group being pushed toward Os, resulting in a bridging configuration. However, it appears that a terminal carbonyl on Rh may be favored by its effectiveness in removing the increased electron density from this metal that has resulted from the electron-donating PMe_3 group. Although **2** rapidly reacts with diazomethane, the isoelectronic species **6**, is unreactive. Clearly, the coordinative unsaturation at Rh, required for reaction with diazomethane, is not readily achieved with this PMe_3 complex.

(c) Ethylene Complexes. Compound **5** reacts rapidly with diazomethane, at temperatures between $-78\text{ }^\circ\text{C}$ and ambient to give the ethylene-containing product $[\text{RhOs}(\eta^2\text{-C}_2\text{H}_4)(\text{CO})_3(\text{dppm})_2][\text{BF}_4]$ (**7a**), shown in Scheme 6. At ambient temperature only one resonance for the ethylene ligand (either ^1H or ^{13}C) is observed owing to facile olefin rotation, whereas, at $-80\text{ }^\circ\text{C}$ two resonances are observed. In the ^1H NMR spectrum at this temperature, the ethylene resonances, at δ 2.13 and 1.12, are broad and no coupling is resolved. When compound **7a** is generated from CH_2N_2 addition to the ^{13}C -labeled **5** ethylene resonances, at δ 36.0 and 13.8 in the $^{13}\text{C}\{^1\text{H}\}$ NMR spectrum, appear as singlets at $-80\text{ }^\circ\text{C}$ with no coupling observed to Rh. This clearly establishes that the ethylene ligand is bound to Os. Furthermore, the high-field ^{13}C chemical shifts for this group are more in line with that expected for an Os-bound group than for a Rh-bound ethylene (see compounds **7b** and **9** for comparison, *vide infra*). In the ^{13}C NMR spectrum of a ^{13}C -enriched sample, a Rh-bound carbonyl resonance is observed at δ 181.9, displaying coupling to Rh (74 Hz) and to the Rh-bound phosphines, a second is observed at δ 184.6, displaying coupling to only the Os-bound phosphines, while a third, at δ 194.6, shows coupling to the Os-bound phosphines and to Rh (4 Hz). This small coupling to Rh, combined with the low-frequency IR stretch at 1906 cm^{-1} suggests a weak semibridging

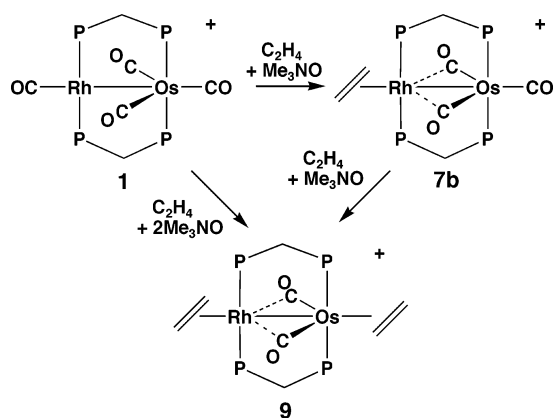
interaction of this carbonyl with Rh. The other carbonyl stretches ($1978, 1959\text{ cm}^{-1}$) are clearly due to terminally bound groups.

Insertion of olefins into a metal–carbon bond of a bridging methylene group to give metal-bound C_3 fragments have been observed 23 or postulated in the generation of higher olefins. 24 Attempts to induce analogous coupling through reaction of **2** with ethylene failed, with no reaction being observed over the temperature range of $-80\text{ }^\circ\text{C}$ to ambient. However, compound **5** reacts with ethylene at $-80\text{ }^\circ\text{C}$ to give the ethylene adduct $[\text{RhOs}(\eta^2\text{-C}_2\text{H}_4)(\text{CO})_3(\mu\text{-CH}_2)(\text{dppm})_2][\text{BF}_4]$ (**8**) as shown in Scheme 6. In addition to the dppm resonances in the ^1H NMR spectrum, the bridging methylene resonance is observed as a broad singlet at δ 5.88, whereas a broad resonance for ethylene is observed between δ 4.5 and 5.0. Although excess ethylene is present, no signal for free ethylene is observed. Instead, the observed signal integrates for both free and coordinated ethylene, indicating facile on/off exchange of this ligand even at $-80\text{ }^\circ\text{C}$. Under these conditions, the ethylene chemical shift is dependent on the ethylene concentration in solution, approaching that for the free ligand (δ 5.39) at high ethylene concentration. The resonance at δ 4.95, reported in Table 1, integrates as four ethylene molecules, indicating that in this experiment there are three equivalents in excess. In the $^{13}\text{C}\{^1\text{H}\}$ NMR spectrum of a ^{13}C -enriched sample, one carbonyl is shown to be bound to Rh (δ 194.3) on the basis of a 60 Hz coupling to this metal, whereas the other two (δ 186.8, 179.8) are terminally bound to Os. Although no spin–spin coupling between the olefin protons and Rh was observed in the ^1H NMR spectrum, owing to the breadth of the signal, the location of two terminal carbonyls on Os and only one on Rh suggests that ethylene is bound at the vacant site on Rh. This would give compound **8** a structure reminiscent of the PMe_3 adduct **6**. Warming a sample of **8** to ambient temperature results in reversion to **5** and free ethylene and maintaining this sample at ambient temperature results in the slow conversion (over several days) to the ethylene-containing product **7a** with accompanying formation of propene. Presumably, ethylene insertion into the Rh– CH_2 bond of **8** occurs, as previously proposed, 24 yielding the propanediyl-bridged intermediate (Scheme 6) which undergoes β -hydrogen elimination to give an allyl hydride species followed by reductive elimination of propene. Reaction of the remaining Rh/Os complex with ethylene presumably yields the ethylene adduct **7a**.

Attempts to generate C_2 -bridged products, related to **7a**, by the reaction of the carbonyl precursor, $[\text{RhOs}(\text{CO})_4(\text{dppm})_2][\text{BF}_4]$ (**1**) with ethylene failed with no reaction observed. However, upon addition of 1 equiv of Me_3NO to a solution of **1** under an atmosphere of ethylene an instantaneous reaction occurs yielding two products, $[\text{RhOs}(\eta^2\text{-C}_2\text{H}_4)(\text{CO})_3(\text{dppm})_2][\text{BF}_4]$ (**7b**) and $[\text{RhOs}(\eta^2\text{-C}_2\text{H}_4)_2(\text{CO})_2(\text{dppm})_2][\text{BF}_4]$ (**9**), together with unreacted **1** (Scheme 7). We were not able to selectively remove a single carbonyl from **1** to give **7b** exclusively, even when less than 1 equiv of Me_3NO was used. Carbonyl loss from **7b** is competitive with CO loss from

- (23) (a) Howard, T. R.; Lee, J. B.; Grubbs, R. H. *J. Am. Chem. Soc.* **1980**, *102*, 6876. (b) Lee, J. B.; Gajola, G. J.; Schaefer, W. P.; Howard, T. R.; Ikariya, T.; Straus, D. A.; Grubbs, R. H. *J. Am. Chem. Soc.* **1981**, *103*, 7358. (c) Motyl, K. M.; Norton, J. R.; Schauer, C. K.; Anderson, O. P. *J. Am. Chem. Soc.* **1982**, *104*, 7325.
- (24) (a) Sumner, C. E., Jr.; Riley, P. E.; Davis, R. E.; Pettit, R. *J. Am. Chem. Soc.* **1980**, *102*, 1752. (b) Theopold, K. H.; Bergman, R. G. *J. Am. Chem. Soc.* **1981**, *103*, 2489. (c) Kao, S. C.; Thiel, C. H.; Pettit, R. *Organometallics* **1983**, *2*, 914.

Scheme 7



compound **1** resulting in competitive formation of the bis-ethylene product. However, **9** can be obtained as the sole product by the addition of two equiv of Me_3NO to **1** under an ethylene atmosphere. Compound **9** shows two ethylene resonances in the ^1H NMR spectrum; a triplet at δ 0.90 displays 6 Hz coupling to the Os-bound phosphines so is clearly due to the Os-coordinated C_2H_4 ligand, and a multiplet resonance at δ 2.89 corresponds to the Rh-bound ethylene group. Selective ^{31}P decoupling experiments shows that this latter ethylene group couples to the Rh-bound phosphines and also allows the observation of a 2 Hz coupling between Rh and these protons. In the ^{13}C NMR spectrum only one carbonyl resonance is observed at δ 195.5, having approximately equal 8 Hz coupling to the Rh nucleus and to the Os-bound phosphines, indicating that both carbonyls are primarily bound to Os, but having a weak semi-bridging interaction with Rh. This semi-bridging formulation is supported by the carbonyl stretch in the IR spectrum at 1858 cm^{-1} . When $^{13}\text{C}_2\text{H}_4$ is used in the preparation of **9**, two ethylene resonances are observed in the ^{13}C NMR spectrum; the high-field resonance at δ 23.5 corresponds to the Os-bound ethylene ligand, and that at δ 64.6, showing 11 Hz coupling to Rh, corresponds to the Rh-bound group. No coupling to phosphorus is observed in either signal.

Although the mono-ethylene product (**7b**) could not be obtained pure, its spectral parameters can be obtained from the mixture of products. In the ^1H NMR spectrum the ethylene resonance appears as a broad unresolved multiplet at δ 2.75. ^{31}P -decoupling experiments confirm the coupling between the ethylene protons and the Rh-bound ends of the diphosphines, and also allow the 2 Hz coupling to Rh to be resolved; both pieces of coupling information indicate that ethylene is bound to Rh. This connectivity is more clearly demonstrated by the ^{13}C NMR spectrum of a $^{13}\text{C}_2\text{H}_4$ -enriched sample which shows the ethylene signal as a doublet at δ 64.2, having 11 Hz coupling to Rh. The carbonyls appear in a 2:1 ratio at δ 198.0 and 181.2, respectively; both signals display coupling to the Os-bound phosphorus nuclei, while the first displays an additional 6 Hz coupling to Rh. Clearly, **7b** and **9** have analogous structures in which the axial site on Os opposite the metal–metal bond is occupied by a carbonyl in **7b** and an ethylene ligand in **9**. These similarities are borne out by the close similarities in many of the spectral parameters of these compounds. It is interesting that the initial replacement of a carbonyl by ethylene occurs at Rh, and that once this substitution occurs the lability of a carbonyl on Os is enhanced. This represents an interesting

example of the trans effect of an ethylene ligand being transmitted through the metal–metal bond. The transmission of the trans effect from one metal to another, via the metal–metal bond, has previously been noted by Oro and co-workers.²⁵

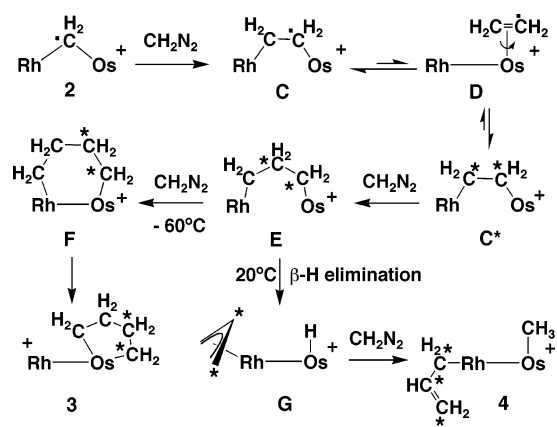
Compound **7b** is an isomer of **7a**, having the ethylene bound to Rh instead of to Os. Clearly, the activation barrier to interchange of these isomers is substantial since interconversion does not occur at ambient temperature. Attempts to establish which of these isomers is thermodynamically favored failed since warming solutions of either in attempts to effect conversion to the favored species resulted in decomposition in both cases. It is also interesting that isomers **7a** and **7b** were ostensibly obtained from the same $[\text{RhOs}(\text{CO})_3(\text{dppm})_2]^+$ precursor. In the first case, this unsaturated complex was presumed to be generated by propene loss from the putative propanediyl intermediate, shown in Scheme 6, whereas in the second case, it was generated by trimethylamine oxide addition to compound **1**. The formation of different isomers under these different conditions indicates that the nature of the unsaturated precursor differs subtly under both sets of conditions.

Discussion

(a) Mechanisms of Methylene Coupling. The observation that $[\text{RhOs}(\text{CO})_4(\text{dppm})_2][\text{BF}_4]$ (**1**) reacts with an excess of diazomethane at ambient temperature to give essentially quantitative conversion to $[\text{RhOs}(\eta^1\text{-C}_3\text{H}_5)(\text{CH}_3)(\text{CO})_3(\text{dppm})_2][\text{BF}_4]$ (**4**), in which an allyl group is bound to Rh and a methyl group is bound to Os, is intriguing and led us to question how the transformation of four methylene groups into the allyl and methyl groups had occurred. In particular, we were interested in establishing the roles of the two different metals in this process. We therefore reinvestigated the reaction of **1** with diazomethane at different temperatures in attempts to observe and characterize additional species that may help elucidate the steps in this unique methylene-coupling reaction. In total, three products of methylene incorporation in this RhOs system have been observed, depending on the temperature, as depicted in Scheme 1. At the lowest temperature investigated ($-80\text{ }^\circ\text{C}$) the incorporation of only one methylene fragment occurs yielding the methylene-bridged product $[\text{RhOs}(\text{CO})_3(\mu\text{-CH}_2)(\mu\text{-CO})(\text{dppm})_2][\text{BF}_4]$ (**2**). This incorporation occurs without carbonyl loss. At intermediate temperatures, between $-60\text{ }^\circ\text{C}$ and approximately $0\text{ }^\circ\text{C}$, a third species, $[\text{RhOs}(\text{C}_4\text{H}_8)(\text{CO})_3(\text{dppm})_2][\text{BF}_4]$ (**3**), is observed in which the condensation of four methylene units to give a butanediyl fragment has occurred. Above $-40\text{ }^\circ\text{C}$, the allyl/methyl species (**4**) begins to appear as a minor product together with **3**, and at temperatures approaching ambient it becomes the sole product. Compounds **3** and **4** do not interconvert at ambient temperature indicating that they are generated from **1** by different reaction pathways. Compound **2** can also be used as the precursor of **3** and **4** by reaction with diazomethane at the temperatures given above, and its isolation has allowed us to carry out isotope-labeling studies by generating the $^{13}\text{CH}_2$ -labeled or CD_2 -labeled compounds, **2- $^{13}\text{CH}_2$** and **2- CD_2** , and following the distribution of the isotopes upon conversion to **3** and **4**. The incorporation of the labeled methylene group of **2** into the products **3** and **4** allows us first to establish that **2** is involved as a probable intermediate in the

(25) Sola, E.; Torres, F.; Jiménez, M. V.; López, J. A.; Ruiz, S. E.; Lahoz, F. L.; Elduque, A.; Oro, L. A. *J. Am. Chem. Soc.* **2001**, *123*, 11 925.

Scheme 8



formation of these products from **1**, and the distribution of the labels in **3** and **4** gives information on how these transformations occur. The sites of isotopic incorporation into these products were shown earlier in Schemes 2 and 3. In both cases some scrambling of the ¹³C and ²H occurred. In all insertion steps we assume that methylene insertion into the Rh-CH₂ bond rather than the Os-CH₂ bond occurs. This proposal is consistent with the results of the labeling study, and can be rationalized on the basis of a predicted weaker Rh-C bond compared to Os-C bond,²⁶ which allows more facile insertion into the Rh-C bond, and on the incipient coordinative unsaturation at Rh, which allows for nucleophilic attack of diazomethane at this metal, followed by N₂ loss, generating a Rh-bound methylene group, which inserts into the Rh-C bond of the bridging hydrocarbyl fragment.

Although the X-ray structural and spectroscopic parameters for **2** indicate a substantial contribution from the carbonyl-bridged canonical form (structure **B** of Chart 1), which would give a saturated 18-electron configuration at both metals, displacement of the bridging carbonyl by nucleophilic attack at Rh still occurs. The susceptibility of the Rh center in **2** to nucleophilic attack is demonstrated by its reaction with PMe₃ resulting in CO loss and accompanying binding of PMe₃ at Rh, adjacent to the bridging methylene group. The failure of this PMe₃ product **5**, which is coordinatively saturated at both metals, to react with CH₂N₂ supports the idea that a site of incipient unsaturation at Rh, presumably resulting from movement of the bridging carbonyl in **2** to a terminal site on Os, much as diagrammed for structure **A** (Chart 1), is necessary.

Additional support for methylene insertion into the Rh-CH₂ bond comes from the reactivities of **2** or **5** and the Rh/Ru analogue with alkynes^{12b,27} and allenes,^{27,28} which give products of insertion into the Rh-CH₂ bond, leaving the Os-CH₂ or Ru-CH₂ bond intact. On the assumption that methylene insertion occurs at Rh, the first product would be an ethylene-bridged structure **C**, shown in Scheme 8, in which the label (¹³C or ²H) has remained adjacent to Os. Note that in this scheme

the sites of label incorporation are shown only for ¹³C. Reversible conversion of a bridging ethylene group into a terminally bound ethylene group has been demonstrated²⁹ and would yield an η²-olefin product, such as **D**. The η² binding mode is known to allow facile rotation about the metal-olefin bond,³⁰ as was demonstrated for compound **7a**, and subsequent reversion to the ethylene-bridged intermediate, would result in scrambling of the label equally over the two CH₂ sites to give **C***. It should also be recalled that ethylene is always obtained in the reaction of either **1** or **2** with diazomethane. Presumably, this occurs by ethylene loss from an intermediate such as **D**, regenerating **1**, which can react with CH₂N₂ regenerating **2**. We have no structural information about the η²-olefin adduct **D**; however, it is shown in Scheme 8 as having ethylene bound to Os, since we have demonstrated that the tricarbonyl ethylene adduct **7a**, generated by the reaction of the methylene-bridged **5** with diazomethane, has the ethylene ligand bound to a site adjacent to the bridging position, much as proposed for **D**.

Methylene insertion into the Rh-CH₂ bond of **C*** would yield the propanediyl-bridged intermediate **E**, examples of which are known^{23c,31} or have been proposed as intermediates in the formation of higher olefins.²⁴ However, none of the previously described C₃-bridged species resulted from the stepwise coupling of methylene groups, as proposed in this study. Subsequent insertion of another methylene group into the Rh-C bond of **E** would yield **F**, which we presume rearranges to the final product **3**, through transformation of the strained six-membered dimetallacycle to the unstrained five-membered osmacycle. Note that stepwise insertion of methylene groups into the Rh-CH₂ bonds of the hydrocarbyl-bridged intermediates, together with ethylene rotation in **D**, rationalizes the sites of label incorporation (both ¹³C and ²H) in compound **3**. The loss of the Rh-CH₂ bond upon migration to Os, yielding **3**, is compensated for by the agostic interaction by this CH₂ group in the final product.

At higher temperatures, we propose that β-H elimination from the central carbon of the propanediyl-bridged fragment in **E** becomes competitive yielding an allyl/hydride complex, one possible isomer of which is shown as **G**, and subsequent methylene insertion into the Os-H bond could give the allyl/methyl complex **4**. The sequence **C*** → **E** → **G** is not unlike that proposed by Pettit and co-workers, for the reaction of [Fe₂(CO)₈(μ-CH₂)] with ethylene,^{24a,c} and by Theopold and Bergman for a similar reaction involving Cp₂Co₂(CO)(μ-CH₂).^{24b} In both cases a C₃H₆-bridged intermediate, analogous to **E**, is proposed to undergo β-hydride elimination to give an allyl/hydride complex, before reductive elimination of propene. The difference observed in our case presumably results from the rapid interception of the hydrido intermediate by an additional methylene group yielding the methyl ligand. Again, this proposal for the formation of **4** is consistent with the labeling study. β-H elimination from the ¹³C-labeled **E** would give an allyl group having equal ¹³C incorporation at one terminal CH₂ group and at the central carbon. Conversion to an η¹-allyl group would give a further isotope dilution at the α and γ sites in **4** since there would be an equal probability of either end of the

(26) (a) Ziegler, T.; Tschinke, V. *Bonding Energetics in Organometallic Compounds*; Marks, T. J., Ed.; American Chemical Society: Washington, DC, 1990; Chapter 19. (b) Ziegler, T.; Tschinke, V.; Ursenbach, B. *J. Am. Chem. Soc.* **1987**, *109*, 4825. (c) Armentrout, P. B. *Bonding Energetics in Organometallic Compounds*; Marks, T. J., Ed.; American Chemical Society: Washington, DC, 1990; Chapter 2.

(27) (a) Chokshi, A. M. Sc. Thesis, University of Alberta, 2004. (b) Rowsell, B. D. Ph.D. Thesis, University of Alberta, 2004.

(28) Chokshi, A.; Rowsell, B. D.; Trepanier, S. J.; McDonald, R.; Cowie, M., submitted for publication.

(29) (a) Bender, B. R.; Ramage, D. L.; Norton, J. R.; Wisner, D. C.; Rappé, A. K. *J. Am. Chem. Soc.* **1997**, *119*, 5628. (b) Johnson, B. F. G.; Lewis, J.; Pippard, D. A. *J. Chem. Soc., Dalton* **1981**, 407.

(30) Collman, J. P.; Hegedus, L. S.; Norton, J. R.; Finke, R. G. *Principles and Applications of Organotransition Metal Chemistry*; University Science Books: Mill Valley California, 1987; pp 523–660.

(31) Theopold, K. H.; Bergman, R. G. *Organometallics* **1982**, *1*, 1571.

allyl group coordinating to the metal. It should also be recalled that **4** is fluxional, and exchange of the α and γ positions of the η^1 -allyl group would also result in scrambling of the label. According to this scheme, no ^{13}C incorporation into the methyl group would occur since this carbon originates from unlabeled diazomethane. By arguments similar to those for ^{13}C scrambling, ^2H scrambling over all allyl positions occurs. In addition, removal of one hydrogen from the central carbon in **E**, a site having ^2H incorporation, will incorporate some ^2H into the hydride group of **G** resulting in ^2H incorporation into the methyl group of **4**.

We have attempted to model the transformation of the allyl hydride intermediate (**G**) to **4** via protonation of the known η^3 -allyl complex, $[\text{RhOs}(\eta^3\text{-C}_3\text{H}_5)(\text{CO})_3(\text{dppm})_2]$, and subsequent reaction with diazomethane. However, protonation of this allyl species, even at -80°C , leads to facile decomposition, and even in the presence of diazomethane, attempted protonation of this allyl species also led to decomposition in which no evidence of either **3** or **4** could be observed.

The formation of **3** is favored at lower temperatures, whereas the formation of **4** becomes favorable at higher temperatures. Unfortunately, the appropriate experiments to determine the activation enthalpies and entropies for the formation of compounds **3** and **4** have not been carried out. One of the major problems in carrying out such a study is the capricious nature of reactions involving diazomethane and these transition-metal complexes. We have found that under seemingly identical conditions the reaction of CH_2N_2 with **1** or **2** can lead to substantial, although variable, amounts of polymethylene and ethylene, which can lead to incomplete formation of the expected products (**3** or **4**) and difficulties in determining the concentration of diazomethane in solution from reaction to reaction.

(b) Models for C₂-Bridged Intermediates. The proposed C₂H₄-bridged intermediate (**C**) in our methylene-coupling sequence is never observed; clearly, once generated, it is rapidly intercepted by reaction with diazomethane yielding **3** or **4** or both. In attempts to obtain ethylene-bridged species directly, three ethylene complexes, **7a**, **7b**, and **9**, have been generated. However none of these products has an ethylene group in the bridging position as suggested for intermediate **C**. Compound **7a**, having the ethylene ligand bound to Os, adjacent to the bridging site, appears to be closest to **C**, but it does not react further with diazomethane. The reasons for this difference in reactivity will be discussed in relation to the stage at which carbonyl loss occurs in the methylene-coupling sequence (vide infra). The other monoolefin isomer, **7b**, does react with diazomethane to yield a mixture of unidentified products, but neither **3** nor **4** is detected in this reaction mixture. Clearly, the binding mode of the ethylene ligand is pivotal in determining the course of the reaction with diazomethane, with an ethylene-bridged product such as **C** being necessary for the formation of other hydrocarbyl-bridged species such as **E** and **F** in subsequent reactions with diazomethane.

Also produced in the reaction generating **7b** is the bis-ethylene adduct, $[\text{RhOs}(\eta^2\text{-C}_2\text{H}_4)_2(\text{CO})_2(\text{dppm})_2][\text{BF}_4]$ (**9**), resulting from removal of an additional CO from **7b** and accompanying reaction with ethylene. The butanediyl complex (**3**) could, in principle, result from coupling of two ethylene ligands, examples of which are well documented.³² Such a coupling is not observed

with **9**. Certainly, the location of the two ethylene ligands at opposite ends of the complex, and the intervening pair of carbonyl groups makes their coupling unlikely. In addition, this bis-olefin complex is unlikely to be an intermediate in the formation of **3** since it is carbonyl deficient. Any attempts to generate a better stoichiometric model of a bis-ethylene, tricarbonyl intermediate, by reaction of **8** with CO led irreversibly to the tetracarbonyl **1**.

(c) Carbonyl Loss. An unanswered problem that remains in the methylene-coupling transformations of the tetracarbonyl precursors **1** and **2** into the tricarbonyl products **3** and **4**, is the stage at which carbonyl loss occurs. The PMe_3 adduct **6** clearly demonstrates substrate coordination at Rh and can be viewed as a model for diazomethane attack on **2**, preceding N₂ loss and subsequent methylene coupling. On the basis that PMe_3 attack on **2** is accompanied by CO loss, it is tempting to suggest that diazomethane attack on **2** also results in CO loss. However, the observation that the methylene-bridged tricarbonyl species **5** reacts with diazomethane to yield the ethylene complex **7a**, but that this species undergoes no further methylene incorporation, seems to rule out carbonyl loss at an early stage in the methylene-coupling sequence (Scheme 8). Compound **7a** appears to be analogous to intermediate **D**, except that in **7a** movement of ethylene back to the bridging site to yield a species such as **C** appears not to occur. We propose that for methylene incorporation to yield C₃ and C₄ products such as compounds **4** and **3**, methylene insertion into the Rh–CH₂ bond of a hydrocarbyl-bridged fragment has to occur. This suggests that intermediate **C** in Scheme 8 is a tetracarbonyl and that the additional carbonyl, compared to the tricarbonyl **7a**, serves to force the ethylene ligand into the bridging site to allow subsequent methylene incorporation to yield the C₃-bridged intermediate **E**. We propose therefore, that carbonyl loss in the generation of compounds **3** and **4** occurs *after* incorporation of the third methylene group.

Conclusions

The Rh/Os complex, $[\text{RhOs}(\text{CO})_4(\text{dppm})_2]^+$ (**1**) has demonstrated a unique ability to couple diazomethane-generated methylene groups to yield the C₃- and C₄-containing products, $[\text{RhOs}(\eta^1\text{-C}_3\text{H}_5)(\text{CH}_3)(\text{CO})_3(\text{dppm})_2]^+$ (**4**) and $[\text{RhOs}(\text{C}_4\text{H}_8)(\text{CO})_3(\text{dppm})_2]^+$ (**3**), respectively. The failure of the analogous Rh/Ru¹² and Ir/Ru¹³ complexes to accomplish this facile coupling suggests that the Rh/Os pair of metals has the right combination of properties that allows binding of the hydrocarbyl fragments while still being labile enough to allow multiple methylene insertions to occur. Clearly, the coordinative unsaturation at Rh and the lability of the Rh–CH₂ bond allows diazomethane coordination and activation at this metal followed by methylene insertion into the Rh–CH₂ bond, while the greater strength of the Os-hydrocarbyl bond appears to be pivotal in retaining the hydrocarbyl fragment, thereby allowing chain growth to occur. This latter feature is particularly important in the ethylene adduct **D**, from which ethylene loss would otherwise stop the methylene-coupling sequence. This chemistry also demonstrates the importance of bridging binding modes of hydrocarbyl fragments in methylene-coupling sequence, and offers support for the methylene-coupling scheme of Dry to rationalize carbon–carbon coupling in Fischer–Tropsch chemistry.⁶ In the Dry proposal, coupling of surface-bound olefin and methylene groups yields a propanediyl-bridged species,

(32) Pillai, S. M.; Ravindranathan, M.; Sivaram, S. *Chem. Rev.* **1986**, *86*, 353.

which by β -hydrogen elimination and subsequent hydrogen transfer back to the resulting allyl group generates a higher olefin. In the Rh/Os chemistry described, the presumed hydrido allyl intermediate (species **G**, Scheme 8) is intercepted by an additional methylene group to give the allyl methyl complex **4**.

Acknowledgment. We thank the Natural Sciences and Engineering Research Council of Canada (NSERC) and the University of Alberta for financial support of this research and

NSERC for funding of the P4/RA/SMART 1000 CCD diffractometer.

Supporting Information Available: Tables of X-ray experimental details, atomic coordinates, interatomic distances and angles, anisotropic thermal parameters, and hydrogen parameters for compounds **2** and **3**. This material is available free of charge via the Internet at <http://pubs.acs.org>.

JA040054Z